

DEVELOPMENT OF SUPERCONDUCTING SPOKE CAVITY FOR ELECTRON ACCELERATORS*

T. Kubo[†], T. Saeki, KEK, High Energy Accelerator Research Organization, Tsukuba, Ibaraki, Japan
 E. Cenni, H. Fujisawa, Y. Iwashita, H. Tongu, Kyoto University, Uji, Kyoto, Japan
 R. Hajima, M. Sawamura, Japan Atomic Energy Agency, JAEA, Tokai, Ibaraki, Japan

Abstract

A 325 MHz superconducting spoke cavity for the electron acceleration is under development to realize a compact industrial-use X-ray source with the laser-Compton scattering. Optimum designs of the spoke cavity have been searched by using the genetic algorithm, and multipactor simulations are currently in progress to finalize the detailed design. In parallel to the design-optimization efforts, studies toward fabrication processes are also being carried out. In this paper, progresses made so far and a current situation are briefly reviewed.

INTRODUCTION

In order to realize an industrial-use laser-Compton scattering compact X-ray source [1], a superconducting cavity [2] for electron acceleration is currently under development [3]. We adopted a 325 MHz superconducting spoke cavity. The spoke cavity has a small diameter around half the wavelength, namely, half a diameter of the elliptic cavity, and make it possible to reduce RF frequency f_{RF} with keeping its compactness. By setting f_{RF} to 325 MHz, Bardeen-Cooper-Schrieffer resistance ($\propto f_{RF}^2$) is reduced [4], and a cavity dissipation at 4 K nearly equals to that of 1.3 GHz elliptic cavity at 2 K. In this paper, efforts for optimizations of cavity design by electromagnetic-field calculations and multipactor simulations are briefly introduced. Attempts to fabricate the spoke cavity, which have just begun, are also presented.

CAVITY DESIGN

In order to design a spoke cavity, we adopted the genetic algorithm (GA) known as a method of multi-objective optimization [3]. Objectives to be minimized are $g_E \equiv E_{peak}/E_{acc}$ and $g_B \equiv B_{peak}/E_{acc}$, where E_{acc} , E_{peak} and B_{peak} are the accelerating field, the peak electric-field and the peak magnetic-field, respectively. The definition of E_{acc} is given by

$$E_{acc} \equiv \frac{\left| \int E_z(z) e^{-i \frac{2\pi z}{\lambda}} dz \right|}{\frac{\lambda}{2} N_{gap}}, \quad (1)$$

where E_z is the electric-field along the beam axis, $\lambda = c/f_{RF}$, and N_{gap} is a number of gap, which equals to a number of spoke +1. The electromagnetic field calculations were carried out by using CST MW studio (MWS). The procedure

* The work is supported by Photon and Quantum Basic Research Coordinated Development Program from the Ministry of Education, Culture, Sports, Science and Technology, Japan.

[†] kubitaka@post.kek.jp

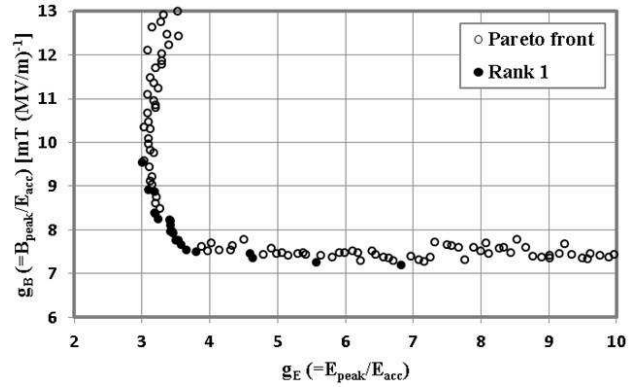


Figure 1: Pareto front shown on the g_E - g_B plane. Each symbol corresponds to an individual.

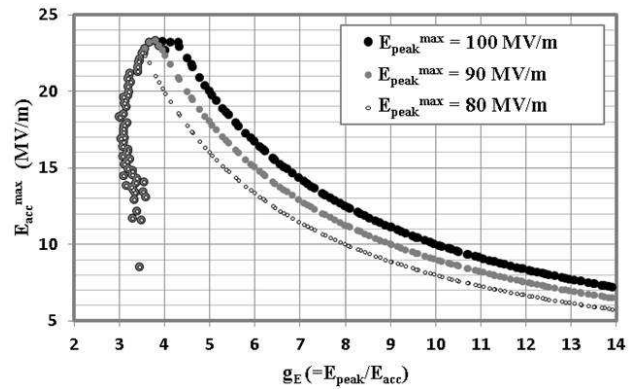


Figure 2: E_{acc}^{max} of individuals on the Pareto front as functions of g_E , where $B_{peak}^{max} = 175$ mT is assumed. Black dots, gray dots and circles correspond to E_{acc}^{max} under assumptions $E_{peak}^{max} = 100, 90, 80$ MV/m, respectively.

is as follows. (i) Generate an initial set of binary data representing geometries of spoke cavities. Binary data and corresponding cavities are called the chromosomes and the individuals, respectively. (ii) Create individuals by decoding chromosomes, and calculate the objectives g_E and g_B . (iii) Evaluate each individual by counting a number of individuals superior to itself (the rank based fitness assignment method), and select parents of the next generation from individuals with better evaluation value or based on a probability varying according to the evaluation value. (iv) Create chromosomes of children from selected parents with uniform crossover method, and mutate them with a fixed probability. (v) Repeat (ii)-(iv) until the improvement of evaluation

Table 1: Parameters of the Optimized Two-Spoke Cavity

Parameter	Value	Unit
Frequency	325	MHz
Cavity diameter	609.5	mm
Cell length	461.2	mm
Cavity length	1383.6	mm
$E_{\text{peak}}/E_{\text{acc}}$	3.7	
$B_{\text{peak}}/E_{\text{acc}}$	7.5	mT/(MV/m)
R/Q	691	Ω
Transit time factor	0.81	

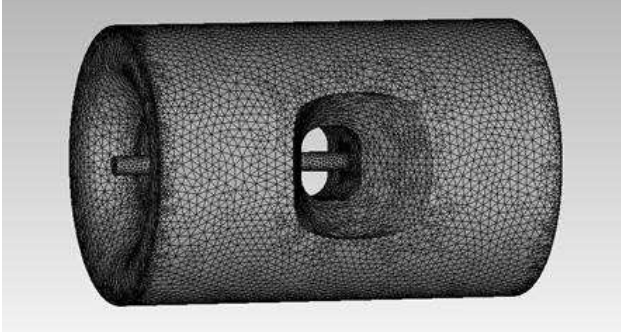


Figure 3: An example of single-spoke cavity.

value steps. Fig. 1 shows the Pareto front of design of the two-spoke cavity obtained by the above procedure.

We can extract individuals that maximize the achievable E_{acc} as follows. Suppose strong electron field emissions (vortex penetrations) are triggered when E_{peak} (B_{peak}) exceeds a threshold value $E_{\text{peak}}^{\text{max}}$ ($B_{\text{peak}}^{\text{max}}$) or E_{acc} exceeds $g_E^{-1} E_{\text{peak}}^{\text{max}}$ ($g_B^{-1} B_{\text{peak}}^{\text{max}}$). Then the achievable E_{acc} of an individual with g_E and g_B can be written as

$$E_{\text{acc}}^{\text{max}} = \min(g_E^{-1} E_{\text{peak}}^{\text{max}}, g_B^{-1} B_{\text{peak}}^{\text{max}}). \quad (2)$$

Fig. 2 shows $E_{\text{acc}}^{\text{max}}$ of individuals on the Pareto front as functions of g_E . At a large g_E region, $E_{\text{acc}}^{\text{max}}$ is limited by $g_E^{-1} E_{\text{peak}}^{\text{max}}$. On the other hand, at a small g_E region, where g_B is large as shown in Fig. 1, $E_{\text{acc}}^{\text{max}}$ is limited by $g_B^{-1} B_{\text{peak}}^{\text{max}}$. Individuals on the Pareto front with $g_E \sim 4$ yield maximum $E_{\text{acc}}^{\text{max}}$ (~ 23 MV/m). Note that the maximum value of $E_{\text{acc}}^{\text{max}} \sim 23$ MV/m is independent of an assumed value of $E_{\text{peak}}^{\text{max}}$ when $E_{\text{peak}}^{\text{max}} > 90$ MV/m. An example of parameters of optimized two-spoke cavity are summarized in Table. 1.

MULTIFACTOR SIMULATION

We plan to fabricate a spoke cavity like Fig. 3, which is a single-spoke version of the cavity designed in the last section. To finalize the detailed design, such as a corner radius of the end plate, we are carrying out multipactor (MP) simulations [5] of models with various corner radii. The procedure is as follows [6]. (i) Calculate the electromagnetic-field distribution by using MWS Eigenmode solver. (ii) Set secondary electron emission (SEE) properties on CST

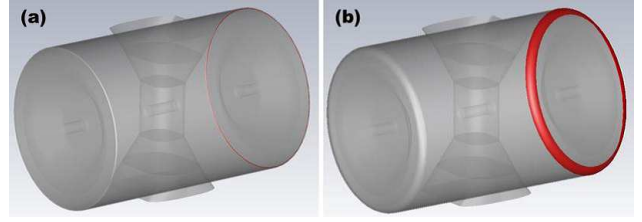


Figure 4: Particle sources (red region) on the corner of (a) Model 1 and (b) Model 5, where the corner radii of Model 1 and Model 5 are 2.8 mm and 25 mm, respectively.

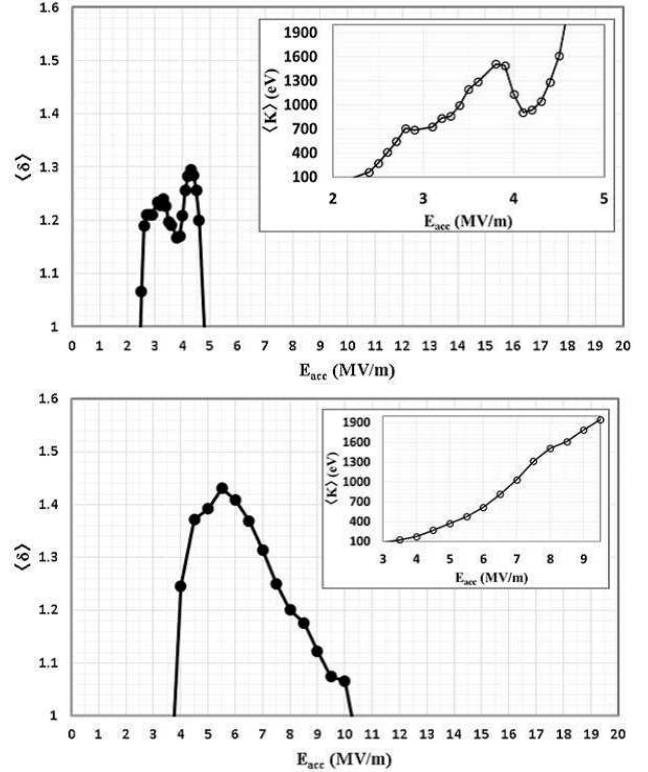


Figure 5: (a) Averaged SEY and averaged impact energy (inset) of Model 1 as functions of E_{acc} obtained by using PS PIC solver. (b) Those of Model 5 obtained by using PS TRK solver. In both cases, 300°C bakeout Nb is used as an SEE material.

Particle Studio (PS). The secondary emission yield (SEY) of a material can be loaded from Material Library. We adopted the Furman model [7] as an SEE model and Nb as a SEE material¹. (iii) Set primary electron (PE) sources. We indicated the corner of the cavity as PE sources (Fig. 4), where a number of PEs and their energies were set to 10^4 and several eV, respectively. (iv) Import the electromagnetic-field obtained at (i) to PS, and simulate electron dynamics in various E_{acc} by using PS TRK solver or PS PIC solver. (v) Repeat the above for other cavities with different geometries.

¹ Three types of Nb are equipped on Material Library: Wet Treatment, 300°C Bakeout, and Ar Discharge Cleaned.

For the MP analysis, the averaged SEY, $\langle\delta\rangle$, and the averaged impact energy, $\langle K\rangle$, are useful [8–10]. $\langle\delta\rangle$ can be calculated by $\langle\delta\rangle = \text{SEE current}/\text{Current}$ [6], where the values named Current and SEE current are given in Collision Information. When MP occurs, $\langle\delta\rangle$ is larger than unity. $\langle K\rangle$ is calculated as $\langle K\rangle = \text{Power}/\text{Current}$ [6], where the value named Power is also given in Collision Information. When MP occurs, $K_1 < \langle K\rangle < K_2$ is satisfied, where K_1 and K_2 are the crossover energies ($\delta(K_1) = \delta(K_2) = 1$). The value of $\langle K\rangle$ reflects the electric-field strength at the area where MP occurs, and is an important clue when we consider changing the cavity geometry to suppress MP [4]. Fig. 5 shows examples of $\langle\delta\rangle$ and $\langle K\rangle$ as functions of E_{acc} . MPs occur at a specific region of E_{acc} , where $\langle\delta\rangle > 1$ and $K_1 \approx 10^2 \text{ eV} < \langle K\rangle < K_2 \approx 2 \times 10^3 \text{ eV}$ are satisfied. At small (large) E_{acc} regions, electrons obtain so small (large) energies that $K < K_1$ ($K > K_2$) and $\langle\delta\rangle < 1$. MP simulations for other models will also be carried out and compared, by which the final design will be fixed.

TOWARD FABRICATION

In parallel to the works on design optimizations, we started to study the fabrication of spoke cavity. Mechanical designs of supporting elements and the vacuum-pressure tolerance simulations are in progress by using the simulation code ABAQUS. We adopt Nb sheets with thickness 3.5 mm as a material of cavity fabrication in view of the simulation results. The cavity will be made up from a number of parts as shown in Fig. 6. Each part will be formed by the press from Nb sheets and welded each other by the electron-beam welding. Press dies are being designed by using a simulation code as shown in Fig. 7.

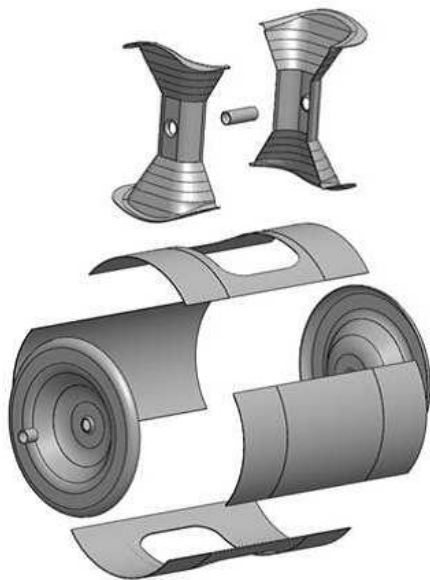


Figure 6: Components of a spoke cavity.

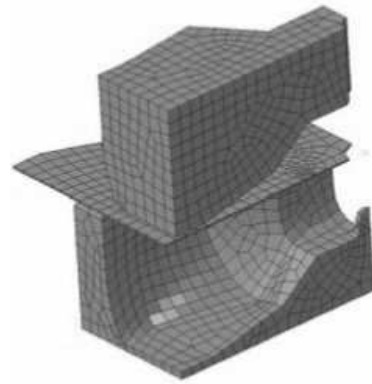


Figure 7: Press simulation of spoke parts carried out by using ABAQUS, where one-fourth of the parts are considered in view of the symmetry.

SUMMARY

We launched a development program of a superconducting spoke cavity for the electron acceleration to realize a compact industrial-use X-ray source with the laser-Compton scattering.

- Spoke cavities were designed by using the genetic algorithm. A set of parameters of optimized cavity are summarized in Table. 1.
- To finalize a detailed design, multipactor simulations of candidate models with different corner radii of end plates are being carried out. We will compare their results and fix the final design.
- Efforts toward fabrication are in progress in parallel to design optimizations. Mechanical designs of supporting elements and the vacuum-pressure tolerance simulations are being carried out. Design of press dies to form components are also in progress.

REFERENCES

- [1] R. Hajima, T. Hayakawa, N. Kikuzawa, and E. Minehara, J. Nucl. Sci. Tech. **45**, 441 (2008).
- [2] C. S. Hopper and J. R. Delayen, Phys. Rev. ST Accel. Beams **16**, 102001 (2013).
- [3] M. Sawamura, R. Hajima, R. Nagai, T. Kubo, H. Fujisawa, and Y. Iwashita, in *Proceedings of IPAC2014, Dresden, Germany* (2014), p. 1946, WEPRO005; M. Sawamura, R. Hajima, R. Nagai, and N. Nishimori, in *Proceedings of SRF2011, Chicago, IL USA* (2011), p. 165, MOPO036;
- [4] H. Padamsee, J. Knobloch, and T. Hays, *RF Superconductivity for Accelerators* (John Wiley, New York, 1998)
- [5] Y. Iwashita, H. Fujisawa, H. Tongu, R. Hajima, R. Nagai, M. Sawamura, and T. Kubo, in *Proceedings of IPAC2014, Dresden, Germany* (2014), p. 2543, WEPRI030.
- [6] G. Romanov, private communications.
- [7] M. A. Furman and M. T. F. Pivi, Phys. Rev. ST Accel. Beams **5**, 124404 (2002).
- [8] G. Romanov, in *Proceedings of LINAC08, Victoria, BC, Canada* (2008), p. 166, MOP043.
- [9] C. S. Hopper and J. R. Delayen, in *Proceedings of LINAC2012, Tel-Aviv, Israel* (2012), p. 303, MOPB056.
- [10] P. Berrutti, T. Khabiboulline, L. Ristori, G. Romanov, A. Sukhanov and V. Yakovlev, in *Proceedings of PAC2013, Pasadena, CA USA* (2013), p. 838, WEPAC23.